

Durham Research Online

Deposited in DRO:

26 May 2020

Version of attached file:

Accepted Version

Peer-review status of attached file:

Peer-reviewed

Citation for published item:

Cruz Victorio, M. E. and Kazemtabrizi, B. and Shahbazi, M. (2020) 'Distributed real-time power management in microgrids using multi-agent control with provisions of fault tolerance.', in 2020 IEEE 29th International Symposium on Industrial Electronics (ISIE) : proceedings. Piscataway, NJ: IEEE, pp. 108-113.

Further information on publisher's website:

<https://doi.org/10.1109/ISIE45063.2020.9152548>

Publisher's copyright statement:

© 2020 IEEE. Personal use of this material is permitted. Permission from IEEE must be obtained for all other uses, in any current or future media, including reprinting/republishing this material for advertising or promotional purposes, creating new collective works, for resale or redistribution to servers or lists, or reuse of any copyrighted component of this work in other works.

Additional information:

Use policy

The full-text may be used and/or reproduced, and given to third parties in any format or medium, without prior permission or charge, for personal research or study, educational, or not-for-profit purposes provided that:

- a full bibliographic reference is made to the original source
- a [link](#) is made to the metadata record in DRO
- the full-text is not changed in any way

The full-text must not be sold in any format or medium without the formal permission of the copyright holders.

Please consult the [full DRO policy](#) for further details.

Distributed Real-Time Power Management in Microgrids Using Multi-Agent Control with Provisions for Fault-Tolerance

Marcos Eduardo Cruz Victorio, Behzad Kazemtabrizi, Mahmoud Shahbazi

Department of Engineering

Durham University

Durham, UK

marcos.e.cruz-victorio@durham.ac.uk

Abstract— This paper presents a distributed real-time control scheme based on multi-agent systems for cost optimisation of a micro-grid using real-time dynamic price estimation. The real-time prices are forecast using realistic UK energy price data via a Markov Chain Monte Carlo algorithm. A backup mechanism for main containers of the agent platform is implemented to improve fault tolerance of the control system, addressing the single point of failure problem at the hardware and software levels. The Multi-Agent system developed in JAVA and run with Raspberry Pi controls a simulated microgrid in an OPAL-RT real-time simulator to test the accuracy of the estimation method, the capacity of the control to realise power management at minimal supply cost, and uninterrupted operation in case of container faults.

Keywords — *Power Management, Multi-Agent, Distributed control, AC Microgrid.*

I. INTRODUCTION

With recent efforts to move towards the smart grid, with more distributed energy resources (DER) connected to the main grid, control systems also have to "reflect" this new nature. To do this, Multi-Agent Systems (MAS) had emerge as a flexible control method that can implement features of centralised and distributed control [1–3], to provide a good level of efficiency and reliability simultaneously.

MAS allows the distribution of the global optimisation problem in smaller problems solved by individual artificial intelligence units known as agents. For example, Energy storage system (ESS) agents may implement energy arbitrage to maximise profit from frequency response services for the UK grid [4]. A microgrid's control is divided in a hierarchy, each level providing references for the level below it. Primary control regulates voltage and frequency of each DER, secondary control regulates power flow within the microgrid and tertiary control regulates the interaction between the microgrid and the main grid. MAS focuses on the secondary and tertiary control [5], mainly dealing with power and State of charge (SoC) management.

When MAS is applied in more distributed controls, with different computers forming a communication network, a combination of protocols are required to realise communication and coordination of the agents and primary control.

This work is supported by the CONACYT-SENER energy sustainability programme with scholarship number 447877 and EU TESTBED Grant Agreement with number 734325.

The Transmission Control protocol (TCP) is used to communicate the "computers" with the primary control and with each other, requiring the definition of Hypertext transfer protocol (HTTP) addresses for each container. The HTTP application is possible through the Message Transport Protocol (MTP) defined by the Foundation of Intelligent Physical Agents (FIPA), to allow transmission of agent communication language (ACL) messages over remote platforms. The remote monitoring agent (RMA), which allows the visualisation of the GUI, also receives messages from the Agent Management System (AMS) from a remote platform to establish a communication for ACL messages across separate hosts [2, 3].

Distributed microgrid control also implies the lack of a central unit casting the price signal to the distributed generators, which creates the need to generate such signal from price estimations, normally found in literature as a combination of probability analysis and artificial intelligence.

Markov Chain Monte Carlo (MCMC) methods, as described in [6], are a common tool for dynamic price forecast in distributed generation. MCMC methods are used in this paper to estimate mean hour price and standard deviation, by Bayes' Rule:

$$P(A/B) = \frac{P(B/A)P(A)}{P(B)} \quad (1)$$

Where $P(A/B)$ is the posterior, $P(B/A)$ is the likelihood, $P(A)$ is the prior, and $P(B)$ is the evidence.

MCMC methods have been used with distributed generation to estimate solar generation [7], and in [8] for wind estimations. In [9, 10], a combined approach of machine learning with maximum likelihood estimation is utilised to predict day ahead market clearing prices, while in [11] scenarios are predicted to minimise total supply cost for a microgrid. In [12] price prediction is used for optimal load control and is established that there is a high correlation of the hour prices of one day and next day, and prices of the same week day.

The rest of the paper is organised as follows: Section II describes the multi-agent system framework used, the restoration service and the specific agents designed and their objectives for the secondary control of the microgrid. Section III details the price estimation method and stop criterion used by the grid agent. Section IV describes the

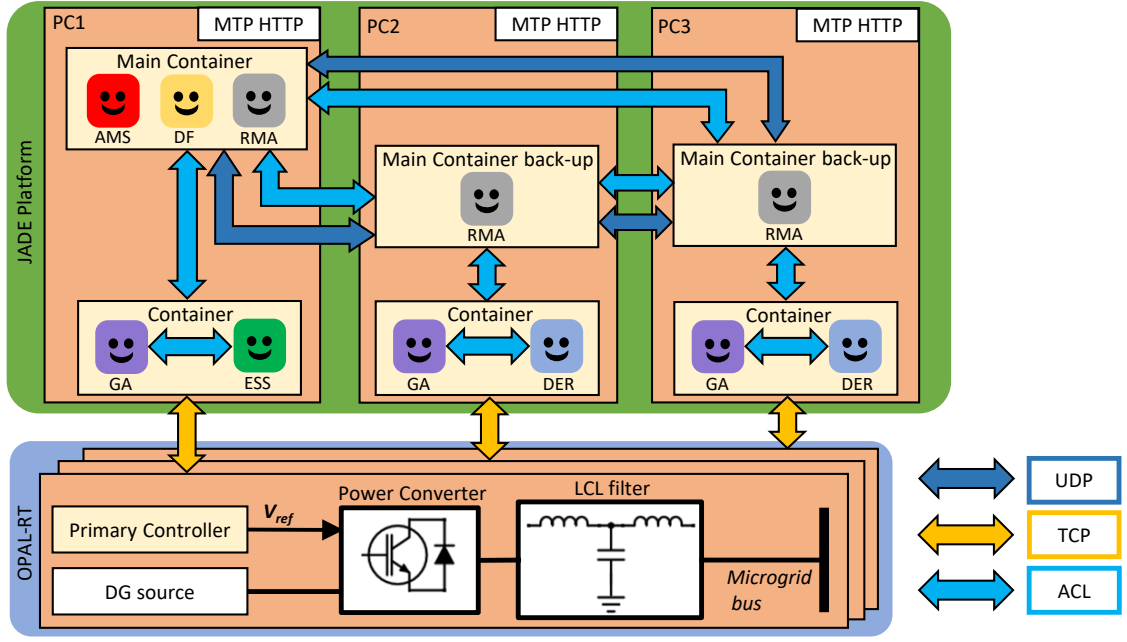


Fig. 1. MAS implementation in simulation for distributed control

test microgrid, supply resources and demand. Section V shows the accuracy and cost results of applying the MCMC method, along with connectivity results of restoration service implemented. Conclusions are presented to summarise the control framework in section VI.

II. MULTI-AGENT SYSTEM CONTROL FRAMEWORK

A MAS programmed with Java Agent Development (JADE) framework is used as a secondary control with the objective of finding optimal power schedule by solving:

$$\min \sum_i \sum_j f_j(P_j(i)), \forall j \in K \wedge \forall i \in N \quad (2a)$$

$$\text{s.t. } P_{jmin} \leq P_j \leq P_{jmax}, \quad (2b)$$

$$L - G = 0, \quad (2c)$$

$$SOC_{min} \leq SOC \leq SOC_{max} \quad (2d)$$

Where j is each source in the set K of total number of sources, i represents each time segment in the set N of total time segments, f_j is the cost function of source j , and $P_j(i)$ is the power from source j at time i , P_{jmin} is the minimum power generation and P_{jmax} is the maximum generation from each source. SOC is state of charge of the ESS. SOC_{min} is the minimum charge and SOC_{max} is the maximum charge.

This is done by breaking the objective in simple tasks that are carried over by individual co-operative agents. The agents output the power references to the primary controllers and price estimations for other agents. In this MAS implementation, the JADE platform is distributed in separate computers. Each computer, or host, holds a main container back-up connected in a ring topology for core services and a container that communicates with the primary control as shown in Fig. 1.

Every JADE platform contain 3 fundamental agents for operation: The Agent Management System (AMS) agent that deals with the creation of agents, Directory Facilitator (DF) agent that coordinate agent service offers and request, and the Remote Monitoring (RMA) Agent which deals with the interface across hosts, which are used in combination with custom agents that will be described in the next section.

In order to make the control resistant to broken communication links or unexpected termination of the containers, User Datagram Protocol (UDP) packet monitoring is implemented. With this service, a hosts is assumed as the main-container and the rests as main-container back-ups, pinging the connection to each other [2]. When the connection is lost for more than 3 seconds, the communication is assumed to be broken and one of the back-ups launches a copy of the AMS and DF and assumes the leadership of the platform, in this way, the fault of any single container will not result in the failure of the entire secondary control. A network can be represented as a graph of vertices in a Laplacian matrix L , with elements:

$$L_{ij} = \begin{cases} |V_i| & i = j \\ -1 & i \neq j \wedge (v_i, v_j) \in E \end{cases} \quad (3)$$

Where V_i is the set of neighbours connected to vertex v_i and E the set of edges connecting 2 vertices, The eigenvalues of L , which are the roots of its characteristic polynomial, or L-polynomial [13], are used to evaluate the connectivity of the MAS. The roots of the L-polynomial are the solutions of:

$$C_G = |L - \lambda I| = 0 \quad (4)$$

In [13] it is mentioned that the number of roots equal to zero in the L-polynomial is equal to the number of separate sub-graphs in the graph, as the L-polynomial is the product of the L-polynomial of the sub-graphs. For the case of the L-polynomial C_G of the union of disjoint of k graphs C_{G_i}

the relationship is described by:

$$C_G = \prod C_{G_i}, \forall i \in k \quad (5)$$

A. Microgrid Agents

1) *Distributed energy resource Agent*: The DER agent, searches for the power schedule that will minimise the total supply cost or maximise profits from trading with the grid.

The affine function is considered for the cost function, along with the start up cost:

$$f_j(P_j(i)) = \begin{cases} BP_j(i) + C + s^* & P_j(i) \neq 0 \\ 0 & P_j(i) = 0 \end{cases} \quad (6)$$

$\forall i \in n \wedge \forall j \in k$

Where the start-up cost function s^* is:

$$s^* = \begin{cases} s & (P_j(i-1) = 0 \wedge P_j(i) > 0) \vee P_j(1) > 0 \\ 0 & otherwise \end{cases}, \quad (7)$$

$\forall i \in n \wedge \forall j \in k$

Where P_j is the power output, B and C are generator specific cost parameters and s is the start-up cost, which is accounted each time its corresponding generator switches on, based on the value of P_j .

The generator starts at any time where the grid price is higher than f , however, an extra condition is considered:

$$\sum_i p(i) - f_j > 0, \forall i \in T \quad (8)$$

Where p is the grid price and T the length of time where the prices crosses the value of f_j . This allows the generators to schedule based on day-ahead price estimations, and minimise costs in the long run.

2) *Energy Storage System Agent*: The objective of the ESS agent is to maximise the benefits from energy arbitrage with the grid. In this case the benefit comes from setting the state of charge in advance such that maximum charge and discharge are available when grid prices are at a local minimum and maximum. The algorithm sets the power references to steer the state of charge to have the required capacity at a particular time. The main constraint of the ESS is the dynamic behaviour of the SoC:

$$SOC_{i+1} = SOC_i - \eta P(i), \forall i \in N \quad (9)$$

The next SoC depends on the previous one and the power $P(i)$ sent or received by the ESS at each time i , multiplied by a constant η , which sets efficiency and capacity.

To realise its objective, the ESS agent looks at the trends of the current grid price and prices in the future, rating the prices to identify its trends and adjust the power reference accordingly.

3) *Grid Agent*: The Grid agent (GA) is created as a request from one of the DER or ESS agent, and registers to the DF to be paired with that agent. The resulting pairs have increased autonomy, compared to having a single GA casting the price signal to all agents. The Grid agent applies the MCMC method to the data of UK hour prices from 16/05/19 to 26/09/19 in

GBP/MWh, obtained from Nord Pool, to obtain the mean and standard deviation of the posterior at each hour for a normal distribution and for each hour of the same weekday, using an heuristic model considering as starting values the hour prices of the previous day as follows:

$$\pi_i = \frac{p_0 + \mu_0 + \mu_1}{3} \quad (10)$$

Where π_i is the MCMC price estimation, p_0 is the price at the same hour of the previous day, μ_0 is the mean MCMC estimation over the entire data of the same hour and μ_1 the mean estimation with the same week day and same hour.

The standard deviation σ_2 used for the confidence interval is calculated as:

$$\sigma_2 = \frac{\sigma_0 + \sigma_1}{2} \quad (11)$$

Where σ_0 is the MCMC estimation using the entire data of the same hour and σ_1 the estimation using the data with the same hour and same week day.

After obtaining the values from the MCMC, the price estimations are send to the DER and ESS agent to be assumed as price signals to realise cost minimisation. The MCMC method is explained in the next section.

III. PRICE ESTIMATION METHOD

To maximise the benefits of the distributed generation, it becomes necessary to interact with the grid such that the total generation cost is minimised. To this, it is necessary to have the spot electricity price in advance to make proper control decisions about the microgrid generators.

The price signal that the agents use to minimise generation costs is estimated using MCMC as described in [6] for the price of each hour of one day.

The method consists on building a Markov chain of proposed parameters θ' to describe the probability density function of the data given a starting vector θ . With a long enough chain, its average converges, obtaining the best approximation of the mean and standard deviation. This represents the Monte Carlo simulation.

A. Metropolis-Hastings method

This MCMC sub method describes the acceptance ratio that generates the elements of the Markov chain.:

$$a = \frac{P(D/\theta')P(\theta')}{P(D/\theta)P(\theta)} \quad (12)$$

Where a is the acceptance, $P(D/\theta')$ is the likelihood of the proposed θ' , given the data D, $P(\theta')$ is the prior on θ' , $P(D/\theta)$ is the likelihood of the current θ and $P(\theta)$ the prior on θ .

Given that the likelihood is computed as the product of all the evaluation of the data under the pdf with the current and proposed parameters, the computation may underflow, so the log-likelihood of the acceptance is taken instead. Then the next element X of the Markov chain is chosen as:

$$X_{i+1} = \begin{cases} \theta' & Z < e^{(Log(a))} \\ \theta & otherwise \end{cases} \quad (13)$$

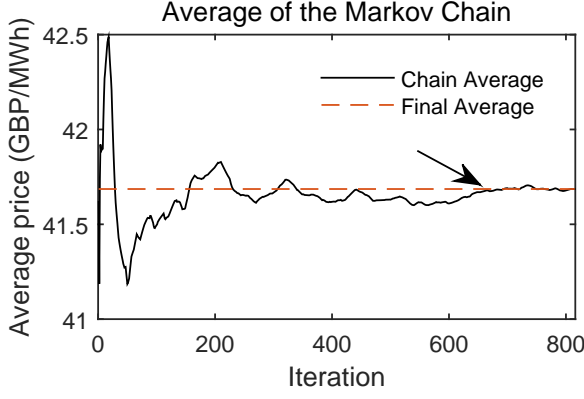


Fig. 2. Evolution of the average of the markov chain for the price of hour 1, the arrow shows the end of the burn-in stage

Where Z is a random number taken from a uniform distribution function. After a long enough chain is generated, the final parameters for the posterior are Monte Carlo approximated as:

$$\theta_f = \frac{1}{n} \sum X_i, \forall i \in n \quad (14)$$

Where n is the number of elements in the chain, and θ_f contains the mean hour price and standard deviation.

B. stop criterion

To optimise computational resources, stop criterion are added to the MCMC method. The stop criteria limits the relative change of the average value of the Markov chain after each iteration to a minimum of $1E-6$, stopping when the following inequality is true:

$$\frac{|\bar{X}_i - \bar{X}_{i+1}|}{\bar{X}_i} < 10^{-6} \quad (15)$$

The first stop criterion is an absolute relative difference between the average of the chain at iteration i , and average of the chain at iteration $i+1$ below $1E-6$, when the proposed value is accepted.

The second stop criterion is reaching maximum cycles per calculated hour price, of 4000 for each model, μ_0 and π_i .

In Fig. 2 the convergence of the average of the markov chain is shown for the price estimation of one hour. The arrow points the end of the burning-in stage, elements in this stage are discarded for the price estimation.

IV. TEST CASE

The microgrid circuit is based on the model proposed in [14], with an ESS and 2 dispatchable generators, a Micro turbine (MT) and a fuel cell (FC) and a varying total demand between 11.22kW and 61.2 kW during the day and its distributed in the circuit as shown in Fig. 3. The Agent platform is deployed using two Raspberry Pi3 model B+ and a PC over a local area network.

The generators parameters are described by table I and the Total demand is found in table II. Table III describes the admittance of the lines.

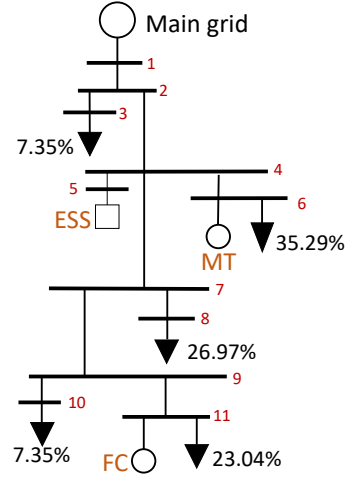


Fig. 3. Microgrid test case and load distribution

TABLE I
DER PARAMETERS

DGU paramter	Micro turbine	Fuel Cell	ESS
P_{min} (kW)	6	6	-30
P_{max} (kW)	30	50	30
b (pence/kWh)	4.37	2.84	0
c (pence)	85.06	255.18	0
s	9	16	0

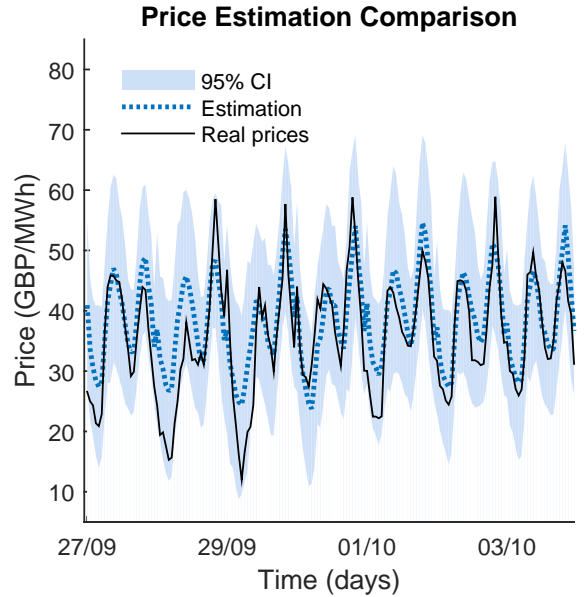


Fig. 4. Comparison of the price estimation for one week.

V. SIMULATION AND RESULTS

A. Price estimation numerical performance

The estimation method is used to generate a price estimation of one week, from the 27/09/2019 to 03/10/2019 showing the estimation and the real prices in Fig. 4. A 95% confidence interval (CI), corresponding to $\pi_1 \pm 1.96\sigma_2$, shows the estimation limits in terms of variations from the mean.

To evaluate the numerical results, two error functions are used [15, 16]:

TABLE II
MICROGRID TOTAL DEMAND

Hour	kW	Hour	kW	Hour	kW	Hour	kW
1	16.32	7	18.36	13	33.66	19	52.02
2	15.30	8	24.48	14	36.72	20	61.20
3	13.26	9	26.52	15	36.72	21	55.08
4	11.22	10	27.54	16	30.60	22	46.92
5	12.24	11	30.60	17	30.60	23	33.66
6	14.28	12	33.66	18	40.80	24	18.36

TABLE III
LINE ADMITTANCE OF THE TEST MICROGRID

Line	Siemens	Line	Siemens
$y_{1,2}$	46.3435 - 13.5440i	$y_{4,7}$	46.3435 - 13.5440i
$y_{2,3}$	9.0275 - 0.2299i	$y_{7,8}$	205.7613 - 205.7613i
$y_{2,4}$	92.6870 - 27.0881i	$y_{7,9}$	3.3505 - 0.0979i
$y_{4,5}$	2.4153 - 0.0143i	$y_{9,10}$	205.7613 - 208.7613i
$y_{4,6}$	17.5886 - 3.6600i	$y_{9,11}$	19.2675 - 2.0134i

$$MAPE = \frac{100\%}{N_e} \sum \left| \frac{p_i - \pi_i}{p_i} \right|, \forall i \in N_e \quad (16)$$

$$RMSE = \sqrt{\frac{1}{N_e} \sum (p_i - \pi_i)^2}, \forall i \in N_e \quad (17)$$

Where RMSE is the root mean squared error and MAPE is the mean absolute percentage error, p_i the real price, π_i the estimated price and N_e the number of estimations.

The table IV summarises the accuracy of the method using the error functions, a comparison is shown between the price signal μ_0 and π_i for the average prices and for the prices of the week 27/09/2019 to 03/10/2019.

B. Costs results

The price π_0 estimated by the MCMC was doubled and tripled to reflect the actual end consumer price, which for the UK was in average 13 pence per kWh in 2019. This is done to better study the effect of the estimation compared to the actual price at the distribution level.

To test the grid price estimation four cases for different prices are used: case 1a is double the average Friday price, case 1b is double the price from 27/09/2019, case 2a is triple the Average Friday price and in case 2b the price is triple the price from 27/09/2019.

Initially, the price signal was developed by a single grid agent and sent to all agents, labelled shared estimation. Secondly the price signal was generated independently in each generator by its own grid agent, labelled as independent estimation, in this way, the distributed generators do not rely on an external signal, however, this produces variations in each forecast.

TABLE IV
SUMMARY OF ACCURACY

Price	Model	MAPE	RMSE
Average	μ_0	0.646%	0.299
	π_i	1.725%	0.824
Week	μ_0	20.335%	7.214
	π_i	15.953%	5.765

Average Supply Cost

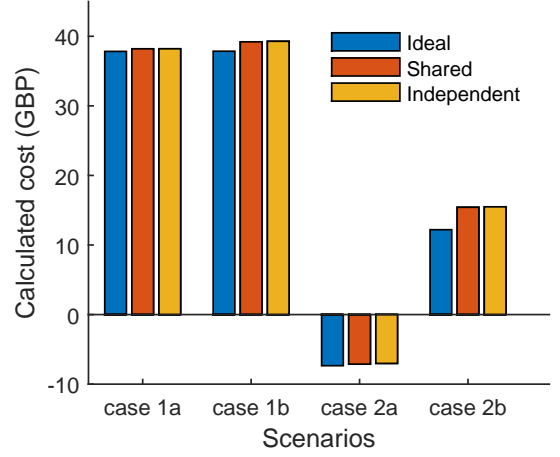


Fig. 5. Comparison of the price estimation strategies

TABLE V
AVERAGE EXTRA COST PER DAY IN GBP

Price	Date	Shared	Independent
Double	Average Friday 27/09/2019	0.373	0.377
		1.347	1.426
Triple	Average Friday 27/09/2019	0.222	0.329
		3.223	3.287

The cost results are summarised in Fig. 5, where each bar represents the average cost after 10 runs for each case. The results are compared with the Ideal case of having the actual prices in each case, showing the extra cost from the estimation in table V. Sharing a single price estimation or using the same data to generate price signals independently does not have a significant effect on the total cost for the test microgrid, but allows further distribution of the control.

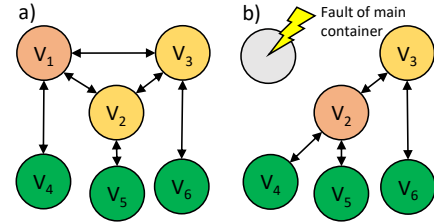


Fig. 6. Graph of the MAS network. a) before and b) after main-container fault in orange, back-ups in yellow, and containers in green.

C. Restoration service

A fault of the main-container is induced in the system to test connectivity of the containers after applying the service restoration, obtaining the L-polynomial of the network from Fig. 1, before and after a fault of the main-container, it can be seen that the network remains fully connected. As depicted in its graph in Fig. 6. Activation of the service is only reflected in the ACL messages from the AMS, as the creation of the copy is informed to other back-ups as shown in Fig. 7. Before the fault the L-polynomial is:

$$\lambda^6 - 6\lambda^5 + 145\lambda^4 - 92\lambda^3 + 69\lambda^2 - 18\lambda = 0 \quad (18)$$

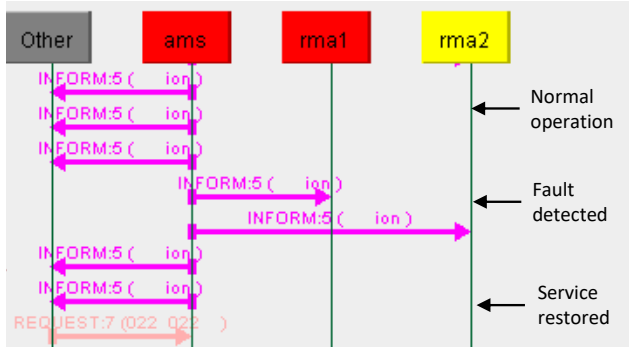


Fig. 7. ACL messages of the AMS showing service restoration.

Which has one root equal to zero. After the fault, the network reforms to exclude the faulty node, with an L-polynomial of:

$$-\lambda^5 + 8\lambda^4 - 24\lambda^3 - 10\lambda^2 + 7\lambda = 0 \quad (19)$$

which also has only one root equal to zero.

VI. CONCLUSION

A price forecast method was tested for the UK market using MAS. While there is opportunity to improve the accuracy of the estimation, the system works in a more distributed environment, which makes it less dependant on a central controller. In the same way, the restoration service prevents the loss of the entire agent platform from the disconnection of the main container. Finally, with a good convergence algorithm, it's possible to distribute the control with independent price estimations, with minimal cost variations.

REFERENCES

- [1] V. N. Coelho, M. W. Cohen, I. M. Coelho, N. Liu, and F. G. Guimaraes, "Multi-agent systems applied for energy systems integration: State-of-the-art applications and trends in microgrids," *Applied Energy*, vol. 187, pp. 820–832, 2017.
- [2] ". Anvari-Moghaddam, A. Rahimi-Kian, M. S. Mirian, and J. M. Guerrero", "A multi-agent based energy management solution for integrated buildings and microgrid system," *Applied Energy*, vol. 203, pp. 41–56, 2017.
- [3] C. Dou and B. Liu, "Multi-agent based hierarchical hybrid control for smart microgrid," *IEEE Transactions on Smart Grid*, vol. 4, no. 2, pp. 771–778, 2013, ISSN: 1949-3061. DOI: 10.1109/TSG.2012.2230197.
- [4] B. Gundogdu, D. Gladwin, and D. Stone, "Battery energy management strategies for uk firm frequency response services and energy arbitrage," *The Journal of Engineering*, vol. 2019, no. 17, pp. 4152–4157, 2019, ISSN: 2051-3305. DOI: 10.1049/joe.2018.8226.
- [5] A. Bidram, A. Davoudi, F. L. Lewis, and Z. Qu, "Secondary control of microgrids based on distributed cooperative control of multi-agent systems," *IET Generation, Transmission Distribution*, vol. 7, no. 8, pp. 822–831, 2013, ISSN: 1751-8695. DOI: 10.1049/iet-gtd.2012.0576.
- [6] J. Harlim, *Data-Driven Computational Methods: Parameter and Operator Estimations*. Cambridge University Press, 2018.
- [7] I. Kim, "Markov chain monte carlo and acceptance-rejection algorithms for synthesising short-term variations in the generation output of the photovoltaic system," *IET Renewable Power Generation*, vol. 11, no. 6, pp. 878–888, 2017, ISSN: 1752-1424. DOI: 10.1049/iet-rpg.2016.0976.
- [8] X. Yang, Y. Yang, Y. Liu, and Z. Deng, "A reliability assessment approach for electric power systems considering wind power uncertainty," *IEEE Access*, vol. 8, pp. 12467–12478, 2020, ISSN: 2169-3536. DOI: 10.1109/ACCESS.2020.2966275.
- [9] C. Wan, Z. Xu, Y. Wang, Z. Y. Dong, and K. P. Wong, "A hybrid approach for probabilistic forecasting of electricity price," *IEEE Transactions on Smart Grid*, vol. 5, no. 1, pp. 463–470, 2014, ISSN: 1949-3061. DOI: 10.1109/TSG.2013.2274465.
- [10] L. Wu and M. Shahidehpour, "A hybrid model for day-ahead price forecasting," *IEEE Transactions on Power Systems*, vol. 25, no. 3, pp. 1519–1530, 2010, ISSN: 1558-0679. DOI: 10.1109/TPWRS.2009.2039948.
- [11] G. Liu, Y. Xu, and K. Tomsovic, "Bidding strategy for microgrid in day-ahead market based on hybrid stochastic/robust optimization," *IEEE Transactions on Smart Grid*, vol. 7, no. 1, pp. 227–237, 2016, ISSN: 1949-3061. DOI: 10.1109/TSG.2015.2476669.
- [12] A. Mohsenian-Rad and A. Leon-Garcia, "Optimal residential load control with price prediction in real-time electricity pricing environments," *IEEE Transactions on Smart Grid*, vol. 1, no. 2, pp. 120–133, 2010, ISSN: 1949-3061. DOI: 10.1109/TSG.2010.2055903.
- [13] D. Cvetković, P. Rowlinson, and S. Simić, "Graph operations and modifications," in *An Introduction to the Theory of Graph Spectra*, ser. London Mathematical Society Student Texts. Cambridge University Press, 2009, pp. 24–51. DOI: 10.1017/CBO9780511801518.003.
- [14] Z. Zhao, "Optimal energy management for microgrids," PhD thesis, Clemson University, 2012.
- [15] G. Li, C. Liu, C. Mattson, and J. Lawarree, "Day-ahead electricity price forecasting in a grid environment," *IEEE Transactions on Power Systems*, vol. 22, no. 1, pp. 266–274, 2007, ISSN: 1558-0679. DOI: 10.1109/TPWRS.2006.887893.
- [16] X. Chen, Z. Y. Dong, K. Meng, Y. Xu, K. P. Wong, and H. W. Ngan, "Electricity price forecasting with extreme learning machine and bootstrapping," *IEEE Transactions on Power Systems*, vol. 27, no. 4, pp. 2055–2062, 2012, ISSN: 1558-0679. DOI: 10.1109/TPWRS.2012.2190627.